PHYSICAL REVIEW D VOLUME 44, NUMBER 6 15 SEPTEMBER 1991

ARTICLES

Solar-neutrino solutions with matter-enhanced flavor-changing neutral-current scattering

V. Barger
Physics Department, University of Wisconsin, Madison, Wisconsin 53706

R. J. N. Phillips
Rutherford Appleton Laboratory, Chilton, Didcot, Oxon, England

K. Whisnant
Physics Department and Ames Laboratory, Iowa State University, Ames, Iowa 50011
(Received 20 May 1991)

We explore quantitatively recent suggestions that the solar-neutrino puzzle may be explained by matter enhancement of nonstandard neutral-current scattering of neutrinos on d quarks. These neutral currents introduce two new parameters, relating to flavor-diagonal and off-diagonal ν-d scattering, which affect the dynamical mixing of two neutrino flavors in the Sun. We consider this mixing in three alternative scenarios: (a) massless neutrinos, (b) massive neutrinos with off-diagonal but no new diagonal currents, and (c) massive neutrinos with both off-diagonal and new diagonal currents. We determine the regions in parameter space that give consistency between the standard solar model and existing solar-neutrino data from the Homestake and Kamiokande-II experiments, and give the corresponding predictions for future experiments with gallium and superfluid helium detectors. We also discuss the more general situation, with nonstandard neutral-current scattering from u quarks and electrons as well as from d quarks, and consider the effects of transmission through the Earth. Finally, we examine the bounds on nonstandard neutral-current neutrino scattering imposed by other experiments; some particular classes of solution are thereby excluded, but a variety of possibilities remains.

I. INTRODUCTION

The long-standing discrepancy between observations of the solar-neutrino flux [1, 2] and expectations from the standard solar model (SSM) [3] has recently received a new type of explanation. It has been proposed [4, 5] that flavor-changing neutral-current (FCNC) and nonstandard flavor-diagonal neutral-current (FDNC) scattering [6] of neutrinos from d quarks in solar matter,

$$\nu_\alpha d \to \nu_\beta d\,, \tag{1}$$

coupled with resonant enhancement [the Mikheyev-Smirnov-Wolfenstein (MSW) effect] [6–12], may be important in explaining the low counting rates in solar-neutrino detectors on Earth. Such neutral-current (NC) effects can arise in supersymmetry models with broken R parity [13]. In this paper we set out to quantify the regions in parameter space where solutions of this new kind can reconcile the present solar neutrino data with the SSM, and to analyze the predictions of these solutions for other neutrino experiments currently in progress or in planning. We analyze the problem in the context of the more general situation, where nonstandard NC scattering from u quarks and electrons,

$$\nu_\alpha u \to \nu_\beta u, \tag{2}$$

$$\nu_\alpha e \to \nu_\beta e, \tag{3}$$

may also occur. In the ensuing discussion, we emphasize the specific case of Eq. (1) but explore also the general features that could occur with Eqs. (2) or (3). We also examine the bounds on nonstandard NC couplings arising from other experiments.

For simplicity, we consider the mixing of just two isospin-doublet neutrino flavors ν_e and ν_α during propagation through solar matter. The formalism can however also be applied when ν_α is a sterile isospin-singlet neutrino [14], by representing the absence of standard NC interactions as the presence of a new FDNC which cancels the standard NC. In the standard electroweak model, the relevant propagation parameters are $\delta m^2 = m_2^2 - m_1^2$ (the difference between the squares of the two vacuum eigenstate masses), θ (the vacuum mixing angle) and $A^W(\nu_e e \to \nu_e e) = -k\sqrt{2}G_F/(2\pi)$ (the spin-averaged amplitude for forward ν_e scattering on electrons due to W exchange where k is the neutrino momentum). Neutral-

current scattering via Z exchange is the same for all doublet neutrino flavors and essentially drops out, giving only an unobservable overall phase. In the presence of additional nonstandard NC scattering from d, u, and e, the corresponding forward-scattering amplitudes $A^{\rm NC}(\nu_\alpha f \to \nu_\beta f)$, $(f = u, d, e)$, also enter the dynamics; they are directly related to the coefficients in the effective Lagrangian describing the new NC interactions (after Fierz reordering, if necessary)

$$-L_{\rm eff} = \sqrt{2}\overline{\nu}_{\alpha L}\gamma_\mu\nu_{\beta L}\left(G^f_{\alpha\beta V}\overline{f}\gamma_\mu f + G^f_{\alpha\beta A}\overline{f}\gamma_\mu\gamma_5 f\right). \tag{4}$$

These new amplitudes contribute to ν_e-ν_α mixing in specific combinations, represented by the following two new parameters per target fermion f:

$$\epsilon_f = A^{\rm NC}(\nu_e f \to \nu_\alpha f)/A^W = G^f_{e\alpha V}/G_F, \tag{5}$$

$$\begin{aligned}\epsilon'_f &= \left[A^{\rm NC}(\nu_\alpha f \to \nu_\alpha f) - A^{\rm NC}(\nu_e f \to \nu_e f)\right]/A^W \\ &= (G^f_{\alpha\alpha V} - G^f_{eeV})/G_F.\end{aligned} \tag{6}$$

The effective axial-vector couplings in Eq. 4 do not contribute to coherent forward scattering. The coupled equations for ν_e and ν_α propagation through matter then have the form

$$i\frac{d}{dt}\begin{pmatrix}\nu_e\\ \nu_\alpha\end{pmatrix} = \begin{pmatrix}0 & \delta m^2\sin 2\theta/(4E_\nu) + B\\ \delta m^2\sin 2\theta/(4E_\nu) + B & \delta m^2\cos 2\theta/(2E_\nu) + C\end{pmatrix}\begin{pmatrix}\nu_e\\ \nu_\alpha\end{pmatrix}, \tag{7}$$

where E_ν is the neutrino energy and

$$B = \sqrt{2}G_F(\epsilon_d N_d + \epsilon_u N_u + \epsilon_e N_e), \tag{8}$$

$$C = \sqrt{2}G_F(\epsilon'_d N_d + \epsilon'_u N_u + \epsilon'_e N_e - N_e). \tag{9}$$

Here N_f denotes the local density of fermion type f in matter; $N_u = 2N_p + N_n$, $N_d = N_p + 2N_n$. The forward amplitudes have opposite sign for neutrino scattering on quarks and antiquarks, so that only the valence-quark densities contribute above. For highly relativistic neutrinos we may set $t = x$ in Eq. (7). Both the broken-R-parity examples [4, 5] and singlet-doublet mixing [14] can be cast in this form.

In the context of supersymmetry models with broken R parity, new neutrino interactions of the following types can occur [13]:

$$\begin{aligned}L_{LLE} = \lambda_{ijk}\Big[&\tilde{e}^j_L\overline{e}^k_R\nu^i_L + (\tilde{e}^k_R)^*(\overline{\nu}^i_L)^c e^j_L \\ &+\tilde{\nu}^i_L\overline{e}^k_R e^j_L - (i\leftrightarrow j)\Big] + \text{H.c.},\end{aligned} \tag{10}$$

$$\begin{aligned}L_{LQD} = \lambda'_{ijk}\Big[&\tilde{d}^j_L\overline{d}^k_R\nu^i_L + (\tilde{d}^k_R)^*(\overline{\nu}^i_L)^c d^j_L + \tilde{\nu}^i_L\overline{d}^k_R d^j_L \\ &-\tilde{e}^i_L\overline{d}^k_R u^j_L - \tilde{u}^j_L\overline{d}^k_R e^i_L \\ &-(\tilde{d}^k_R)^*(\overline{e}^i_L)^c u^j_L\Big] + \text{H.c.},\end{aligned} \tag{11}$$

where i, j, k are generation indices (=1,2,3); see Ref. [15] for a recent discussion. The λ_{ijk} in Eq. (10) are antisymmetric in the first two indices, and we adopt the convention that $\lambda_{ijk} = 0$ for $i \geq j$. These interactions can give rise to ν-d and ν-e scattering, via d-squark and selectron exchange processes, respectively, if the necessary couplings λ_{ijk} and λ'_{ijk} are nonzero. For example [4], λ'_{131} and λ'_{331} together contribute the effective interaction (after Fierz reordering)

$$\begin{aligned}-L_{\rm eff} = &\frac{|\lambda'_{131}|^2}{2m^2_{\tilde{b}}}\overline{\nu}_{eL}\gamma_\mu\nu_{eL}\overline{d}_R\gamma^\mu d_R \\ &+\frac{|\lambda'_{331}|^2}{2m^2_{\tilde{b}}}\overline{\nu}_{\tau L}\gamma_\mu\nu_{\tau L}\overline{d}_R\gamma^\mu d_R \\ &+\frac{\lambda'_{131}\lambda'_{331}}{2m^2_{\tilde{b}}}(\overline{\nu}_{eL}\gamma_\mu\nu_{\tau L}\overline{d}_R\gamma^\mu d_R \\ &+\overline{\nu}_{\tau L}\gamma_\mu\nu_{eL}\overline{d}_R\gamma^\mu d_R),\end{aligned} \tag{12}$$

via b-squark exchange, for neutrino energies much smaller than the b-squark mass $m_{\tilde{b}}$. A typical FCNC diagram is shown in Fig. 1. In this particular case the parameters ϵ_d and ϵ'_d are given by

$$\epsilon_d = \frac{\lambda'_{331}\lambda'_{131}}{4\sqrt{2}G_F m^2_{\tilde{b}}}, \tag{13}$$

$$\epsilon'_d = \frac{|\lambda'_{331}|^2 - |\lambda'_{131}|^2}{4\sqrt{2}G_F m^2_{\tilde{b}}}. \tag{14}$$

Values of ϵ_d and ϵ'_d up to order 1 are allowed in some cases [4, 5, 15]. Similarly this model may have ϵ_e and ϵ'_e from an effective ν-e interaction, but the constraints on the λ and λ' couplings which lead to this interaction are typically more severe than for the constraints on the ν-d couplings (see Sec. V).

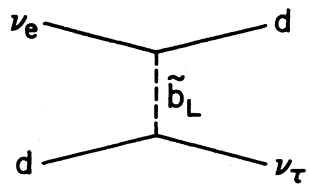

FIG. 1. Squark exchange diagram which contributes to the $\nu_e d \to \nu_\tau d$ flavor-changing neutral current.

In the following sections we principally consider FCNC and new FDNC scattering from d-quarks, since an explicit model has recently been proposed for this case [4, 5], and the couplings are not tightly constrained. We quantitatively explore the implications for present and pending solar neutrino experiments in three alternative scenarios: (a) massless neutrinos ($\delta m^2 = 0$), discussed in Sec. II, and massive neutrinos ($\delta m^2 \neq 0$), both (b) with new FDNC (Sec. III) and (c) without new FDNC (Sec. IV). In each scenario, MSW resonant effects can give large enhancements of $\nu_e \rightarrow \nu_\alpha$ transmutation, but the resonance condition is determined by different factors in each case. In case (a) a resonance occurs if the ratio N_n/N_e (which varies within narrow limits in the Sun) crosses a critical value determined by the ϵ'_f. In case (b), which is similar to the standard MSW effect, a resonance occurs if the value of N_e crosses the standard MSW critical density determined by δm^2, $\sin^2 2\theta$ and E_ν. Case (c) combines the properties of the other two scenarios; depending on the model parameters, it is possible to have two resonance layers in the Sun. The innermost resonance is primarily due to the relative change of N_n and N_e, while the outermost resonance occurs when a particular linear combination of N_n and N_e crosses the standard MSW critical density.

For FCNC and new FDNC ν-d scattering in cases (a) and (b) we determine regions of parameters that give agreement with present data from the Homestake ^{37}Cl experiment [1] and the Kamiokande-II ν-e scattering detector [2], and delineate the implications for the two ^{71}Ga detectors [16, 17] and for a proposed new superfluid ^{4}He detector [18]. For case (c) we indicate how the solutions can be found; they often reduce to a simpler scenario. In each mass scenario, we also consider the general features of FCNC and new FDNC scattering from u quarks and electrons, and discuss the effects of transmission through the Earth.

In Sec. V we discuss limits on FCNC and FDNC parameters from data. In Sec. VI we give a final overview and discussion.

II. MASSLESS NEUTRINOS

Here we assume $\delta m^2 = 0$; strictly speaking, this covers not only massless neutrinos, but also degenerate massive neutrinos and the case where nonstandard NC contributions dominate the standard propagation equations. In this scenario the vacuum mixing parameters δm^2 and θ play no role; neutrino mixing relies entirely upon the parameters ϵ_f and ϵ'_f. An important property of the propagation equations is that they are now independent of neutrino energy [4, 6]. For clarity of presentation we first concentrate attention on the effects of NC scattering in the Sun; in a separate subsection we discuss the small corrections that can arise from NC scattering in the Earth. We also point out some possible Earth effects on atmospheric and accelerator fluxes.

A. ν-d FCNC and FDNC only

We first consider the case where nonstandard NC scattering appears in the ν-d sector alone (the main features of this scenario have been discussed in Ref. [4]). Since $N_p = N_e$ (matter is electrically neutral in the Sun), the propagation equations become

$$i\frac{d}{dx}\begin{pmatrix}\nu_e\\ \nu_\alpha\end{pmatrix} = \sqrt{2}G_F\begin{pmatrix}0 & B\\ B & C\end{pmatrix}\begin{pmatrix}\nu_e\\ \nu_\alpha\end{pmatrix} = \sqrt{2}G_F\begin{pmatrix}0 & \epsilon_d(N_e+2N_n)\\ \epsilon_d(N_e+2N_n) & \epsilon'_d(N_e+2N_n)-N_e\end{pmatrix}\begin{pmatrix}\nu_e\\ \nu_\alpha\end{pmatrix}. \quad (15)$$

For antineutrinos there is an overall sign change, but the relative signs (and hence the propagation) remain the same. The condition for a resonance in matter is that the diagonal elements of the propagation matrix are equal, which in this case means $C = 0$ and hence

$$\epsilon'_d = N_e/(N_e + 2N_n). \quad (16)$$

The ratio on the right-hand side of Eq. (16) rises from a value about 0.5 at the solar center to about 0.75 at the surface. We immediately see that resonant enhancement of $\nu_e \rightarrow \nu_\alpha$ transmutation, normally required to explain the substantial deficit in the observed ν_e flux [1, 2], will only be possible in this narrow range of the parameter ϵ'_d.

The rotation angle θ_m that diagonalizes the matter propagation matrix in Eq. (15) is given by

$$\tan 2\theta_m = \frac{2\epsilon_d(N_e+2N_n)}{\epsilon'_d(N_e+2N_n)-N_e}. \quad (17)$$

If $\epsilon'_d \gg \epsilon_d$ the propagation eigenstates far from resonance will be close to the weak eigenstates ν_e and ν_α, and then adiabatic propagation, though a resonance, will give almost complete conversion of ν_e into ν_α. If ϵ_d is too small, however, the transition will become non-adiabatic and the conversion less complete. And if ϵ_d is too large the resonance will become wide; only a small range of angles θ_m will be traversed and again the $\nu_e \rightarrow \nu_\alpha$ conversion will be reduced. We thus expect that sufficient suppression of the solar ν_e flux will only be obtainable in a restricted range of parameter ϵ_d too.

In general, the probability for ν_e remaining ν_e in the Sun, averaged over an oscillation, is

$$\overline{P}(\nu_e \rightarrow \nu_e) = \tfrac{1}{2}\left[1 + (1-2P_x)\cos 2\theta_m^o \cos 2\theta_m^s\right], \quad (18)$$

where θ_m^o and θ_m^s are the neutrino mixing angles in matter at the neutrino origin and the solar surface, respectively, and P_x is the transition probability for jumping from one eigenstate to the other. There are no more os-

cillations once the neutrino leaves the Sun and enters the vacuum.

Although Eq. (15) is not standard MSW propagation [e.g., the off-diagonal term is not constant in the (ν_e, ν_α) basis], if ϵ_d is small compared to ϵ'_d, then the resonance will be narrow and the off-diagonal term will be approximately constant in the critical resonance region. Then P_x should be given approximately by the standard Landau-Zener transition probability [9]

$$P_x = e^{-\gamma_c \pi/2}, \tag{19}$$

where γ_c is the adiabaticity parameter [4]

$$\gamma_c = \left|\frac{4B^2}{dC/dx}\right|_{\rm res} = \sqrt{2} G_F \left|\frac{N_e}{d(N_n/N_e)/dx}\right|_{\rm res} \frac{2}{\epsilon'_d}\left(\frac{\epsilon_d}{\epsilon'_d}\right)^2 . \tag{20}$$

If $\gamma_c \gg 1$ then the propagation is adiabatic ($P_x \approx 0$). For resonances occurring near the solar center the propagation is non-adiabatic only for small ϵ_d. For example, $\gamma_c < 1$ ($P_x > 0.2$) only when ϵ_d is below approximately 0.004. Thus, the narrow resonance approximation should be valid there. For resonances near the surface, N_n/N_e approaches a constant value and the propagation becomes adiabatic.

We calculated the oscillation probabilities in the usual way [12] using these modified formulas, and found the complete region in the space of parameters ϵ'_d, ϵ_d that will reproduce the mean counting-rate suppressions $R =$ (observed rate)/(SSM rate) of the ^{37}Cl and Kamiokande-II experiments, namely [1, 2]

$$R_{\rm Cl} = 0.27 \pm 0.05, \qquad R_{\rm KII} = 0.46 \pm 0.09, \tag{21}$$

where the experimental and theoretical errors have been added in quadrature. Our results are shown in Fig. 2(a); the shaded area denotes the region that fits the numbers in Eq. (21) within 95% confidence. These results can be understood qualitatively as follows.

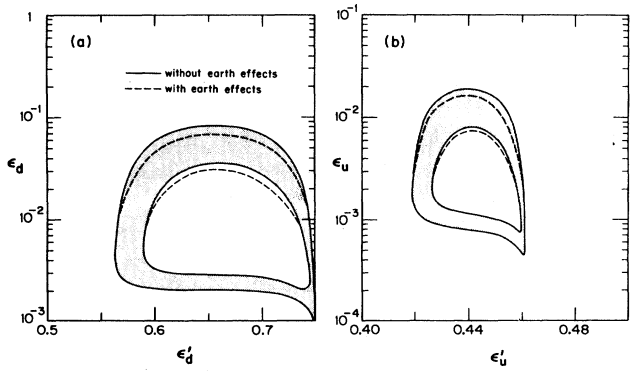

FIG. 2. Solutions to the solar puzzle in the space of parameters (ϵ', ϵ) for nonstandard (a) ν-d and (b) ν-u NC scattering, with massless neutrinos. The shaded region is consistent with the data of Eq. (21) within two standard deviations (95% C.L.), neglecting small Earth effects. The dashed curves show the approximate change in the allowed region when neutrino scattering in the Earth is also taken into account.

(i) For $\epsilon'_d \approx 0.5$, the resonance is at the solar center; no neutrinos can traverse it, so insufficient ν_e conversion occurs.

(ii) For $\epsilon'_d \approx 0.57 - 0.59$, the resonance occurs at a suitable radius where precisely the right fraction of ν_e transmute into ν_α (with adiabatic conversion). This explains the left-hand vertical band in Fig. 2(a).

(iii) For $\epsilon'_d \approx 0.60 - 0.73$, the resonance occurs at a larger radius and adiabatic conversion gives too many $\nu_e \to \nu_\alpha$ transitions.

(iv) For $\epsilon'_d \approx 0.73 - 0.75$, the resonance occurs near the outer radius of the Sun and cannot be fully traversed, making adiabatic conversions less complete and reducing $\nu_e \to \nu_\alpha$ transitions enough to fit Eq. (21) once more. This explains the right-hand vertical band of solutions.

(v) For the other parameter ϵ_d, we have already noted that adiabatic conversion breaks down at sufficiently small values, while the resonance becomes broad at large values. Both these effects reduce the $\nu_e \to \nu_\alpha$ conversion efficiency (which is otherwise too high for $0.60 \le \epsilon'_d \le 0.73$) and lead to the horizontal bands of solutions that bridge between the vertical bands in Fig. 2(a).

Predictions for the counting rate in gallium detectors [16, 17], corresponding to this region of solutions, are shown in Fig. 3 in solar neutrino units (SNU = captures/10^{36}atoms s). We see that a range of gallium rates from about 30 to 90 SNU is indicated, to be compared with the value 132 SNU for the SSM [3]. An accurate measurement of the gallium rate would greatly constrain (or even possibly exclude) this scenario.

Although the propagation equations are independent of energy, the various processes in the Sun that generate neutrinos have different radial distributions, so there can be different degrees of suppression for different energies. Generally the higher energy neutrinos from the Sun

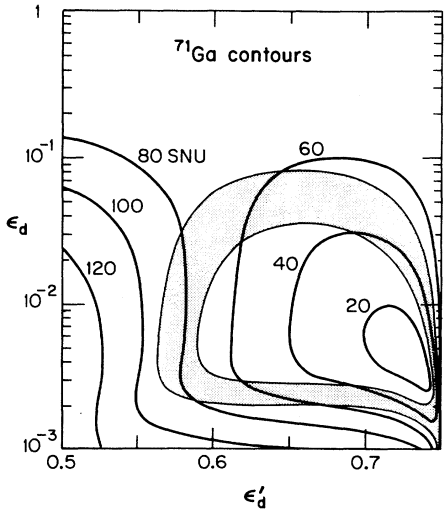

FIG. 3. Predictions of the solar neutrino counting rate in gallium detectors for the ν-d NC solutions of Fig. 2(a), neglecting Earth effects. The contours in the parameter plane correspond to the specified rate in SNU; the shaded area indicates the solution region.

come from smaller radii and hence may be suppressed more than the lower energy neutrinos if the resonance lies between the production radii of the lower- and higher-energy neutrinos. This effect can be quite pronounced; for example, with $\epsilon'_d = 0.58$ and $\epsilon_d = 0.01$ the ^{71}Ga prediction, dominated by lower-energy p-p neutrinos, is 80 SNU (representing a suppression factor of about 0.6), while for ^{37}Cl, dominated by higher-energy ^{8}B neutrinos, the suppression factor is about 0.3.

Figure 4 shows the predicted suppression ratio $R_{\rm He}$= (measured rate)/(SSM rate) for the proposed cryogenic ^{4}He detector [18]. This device would essentially measure the total ν-e scattering rate above some low threshold for detecting scattered electrons. The energy-independence of Eq. (7) means that the suppression ratio of a given source of neutrinos (e.g., the p-p reaction) does not depend on the threshold value. The threshold is important only to the extent that it affects the relative contribution of different neutrino sources. For electron detection thresholds below 50 keV, the threshold effect is at most a few per cent. In addition, there are NC contributions to the signal from ν_α-e scattering; the NC/CC ratio is not very sensitive to the threshold, either. We have included these NC contributions in our calculations of $R_{\rm He}$. We see that a range of $R_{\rm He}$ suppression factors 0.4–0.8 is admissible. An accurate measurement of $R_{\rm He}$ would again greatly constrain the parameters.

Although the contours in Figs. 3 and 4 look rather similar, they actually represent rather different degrees of suppression; e.g., the $R_{\rm He}$=0.5 contour lies very close to the gallium 40 SNU contour, but the latter represents a gallium suppression factor close to 0.3. Much of this difference in suppression ratio comes from the ν_α-e neutral current interactions that raise the signal in ^{4}He but not in ^{71}Ga.

These massless neutrino oscillations could be distinguished from standard MSW oscillations by combining results from several solar neutrino experiments and by the fact that the oscillations depend on the neutrino source but not the neutrino energy. For example, detectors which plan to measure high-energy ^{8}B neutrinos, such as SNO [20], Super-Kamiokande [21], and BOREX [22], would see a uniformly suppressed spectrum.

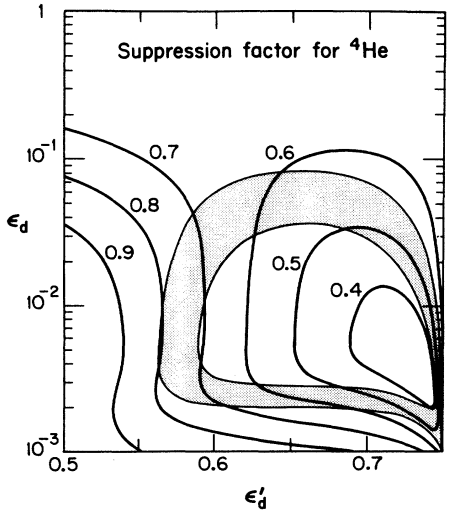

FIG. 4. Predictions of the suppression ratio $R_{\rm He}$ in a superfluid ^{4}He detector for the ν-d NC scattering solutions of Fig. 2(a), neglecting Earth effects. The contours in the parameter plane correspond to constant values of $R_{\rm He}$; the shaded area indicates the solution region.

B. ν-u FCNC and FDNC only

We next consider the case where nonstandard NC scattering occurs in the ν-u sector alone. The propagation equations now become

$$i\frac{d}{dx}\begin{pmatrix}\nu_e\\ \nu_\alpha\end{pmatrix} = \sqrt{2}G_F\begin{pmatrix}0 & \epsilon_u(2N_e+N_n)\\ \epsilon_u(2N_e+N_n) & \epsilon'_u(2N_e+N_n)-N_e\end{pmatrix}\begin{pmatrix}\nu_e\\ \nu_\alpha\end{pmatrix}; \tag{22}$$

the resonance condition is

$$\epsilon'_u = N_e/(2N_e+N_n), \tag{23}$$

and the mixing angle in matter is

$$\tan 2\theta_m = \frac{2\epsilon_u(2N_e+N_n)}{\epsilon'_u(2N_e+N_n)-N_e}. \tag{24}$$

The ratio on the right-hand side of Eq. (23) rises from about 0.40 at the center of the Sun to about 0.46 at the edge, so resonance-enhanced solutions are possible only in this narrow window of ϵ'_u. The allowed region consistent with the solar data is shown in Fig. 2(b); it is an annular region analogous to that for ν-d scattering [Fig. 2(a)], but more constricted in both the horizontal and vertical scales. The adiabaticity parameter γ_c is given by Eq. (20) multiplied by a factor of 2 and with $(\epsilon_d, \epsilon'_d)$ replaced by $(\epsilon_u, \epsilon'_u)$. Since the resonance occurs at a smaller value of ϵ'_u than for ϵ'_d, the non-adiabatic solution band is lower in ϵ_u than for ϵ_d. Also, the mixing angle θ_m is less sensitive to changes in N_n/N_e, so there is a resonance-broadening effect in the adiabatic region that lowers the top horizontal band as well.

C. ν-e FCNC and FDNC only

We next consider the case where nonstandard NC scattering occurs in the ν-e sector alone. The propagation equations now become

$$i\frac{d}{dx}\begin{pmatrix}\nu_e\\ \nu_\alpha\end{pmatrix} = \sqrt{2}G_F N_e\begin{pmatrix}0 & \epsilon_e\\ \epsilon_e & \epsilon'_e-1\end{pmatrix}\begin{pmatrix}\nu_e\\ \nu_\alpha\end{pmatrix}. \tag{25}$$

The matter mixing angle is given by

$$\tan 2\theta_m = \frac{2\epsilon_e}{\epsilon'_e - 1}, \tag{26}$$

independent of solar radius, so there is no possibility of neutrinos traversing a resonance on the way out. There will be ν_e-ν_α oscillations in the Sun, independent of energy, with a wavelength $\lambda = \pi \sin 2\theta_m/(\sqrt{2}G_F N_e \epsilon_e)$ that varies with the electron density. The probability of initial ν_e's remaining ν_e as they traverse the Sun is

$$P(\nu_e \to \nu_e) = 1 - \sin^2 2\theta_m \sin^2 \frac{\psi}{2}, \tag{27}$$

where

$$\psi = \sqrt{4\epsilon_e^2 + (\epsilon'_e - 1)^2}\sqrt{2}G_F \int N_e dx \tag{28}$$

is the relative phase between the two matter eigenstates, which is simply the difference between the eigenvalues in Eq. (25) integrated over the distance traveled. If there are many oscillations on the way out [i.e., $4\epsilon_e^2+(\epsilon'_e-1)^2$ is not too small], the average of these oscillations will give $\overline{P}(\nu_e \to \nu_e) = 1 - \frac{1}{2}\sin^2 2\theta_m \geq \frac{1}{2}$ for all energies, which cannot fit the data in Eq. (21).

An interesting class of possibilities remains. Suppose that mixing is near maximum (ϵ'_e near 1) and the centrally emitted ν_e go through a half integer number of oscillations [$\psi \approx (2n+1)\pi$] with n small. Then ν_e emitted near the solar center would have evolved almost entirely into ν_α at the solar surface; the ν_e flux from ^{8}B that dominates the SSM predictions for the Homestake and Kamiokande-II rates comes from close to the center and would be greatly suppressed. Such oscillations could indeed explain the data of Eq. (21). They are somewhat analogous to the vacuum long-wavelength oscillation solutions [19] to the solar puzzle; however, the latter oscillations have wavelengths of order the Earth-Sun distance, whereas the present matter oscillations have wavelengths of order the solar radius. Note, however, that the net suppression of ν_e now depends on energy in a more complicated manner. Neutrinos from lower-energy sources that are more widely dispersed in the Sun would have a wider range of propagation distances in solar matter; averaging over this range of distances would give less suppression.

D. ν_e regeneration in the earth

In the standard MSW effect there is a range of neutrino parameters for which a substantial fraction of neutrinos that undergo the transition $\nu_e \to \nu_\alpha$ in the Sun change back to ν_e when they pass through the Earth [23, 24]. Here we investigate the effect of the Earth on oscillations of massless neutrinos with nonstandard neutral currents. We find that there is a non-negligible effect, but it is not as pronounced as in the standard MSW scenario. To be specific, we discuss in detail the scenario with ν-d NC only.

Since $N_n/N_e \approx 1$ everywhere in the Earth, the mixing angle is a constant

$$\tan 2\theta_m^e = \frac{6\epsilon_d}{3\epsilon'_d - 1}. \tag{29}$$

Since a resonance in the Sun occurs only for $0.50 < \epsilon'_d < 0.75$, we see that there cannot be a resonance in the Earth for parameters which explain the solar neutrino deficit. Hence, for a solar solution, mixing in the Earth can be sizeable only when ϵ_d is not small, i.e., when the propagation in the Sun is adiabatic. Therefore if θ_m^o and θ_m^s are the mixing angles in matter at the solar neutrino origin and solar surface, respectively [calculated from Eq. (17)], then the probability that an initial ν_e is a ν_e when it reaches the detector may be written as

$$\begin{aligned}\overline{P}(\nu_e \to \nu_e) &= \tfrac{1}{2}\{1 + \cos 2\theta_m^o[\cos 2\theta_m^e \cos 2(\theta_m^s - \theta_m^e) \\ &\quad - \sin 2\theta_m^e \sin 2(\theta_m^s - \theta_m^e)\cos 2\phi]\},\end{aligned} \tag{30}$$

where

$$\phi = \sqrt{36\epsilon_d^2 + (3\epsilon'_d - 1)^2}\sqrt{2}G_F \int N_e dx, \tag{31}$$

represents the relative phase between diagonal eigenstates accumulated during transmission through the Earth. Equation (30) was obtained by rotating to the diagonal basis at the neutrino origin (by the angle θ_m^o), propagating adiabatically through the Sun, rotating back to the weak eigenstates at the solar surface (by the angle θ_m^s), repeating the process for the Earth (where both the initial and final angles are θ_m^e), and then averaging over the relative phase between diagonal eigenstates in the Sun.

The angle ϕ will depend on both the time of day and time of year. For a given day it reaches its maximum value at midnight; for typical ϵ'_d, which solve the solar puzzle, the midnight value of 2ϕ ranges from approximately 10 radians in the summer to 40 radians in the winter at the Homestake detector (43° latitude). On a given night, the value of 2ϕ ranges from zero to its maximum value. Thus at night the $\cos 2\phi$ term in Eq. (30) will be greatly suppressed by averaging, especially if results from different seasons are included together. In addition, because the mixing angle in the Earth θ_m^e is nonmaximal, the $\cos 2\phi$ term is further suppressed by the factor $\sin 2\theta_m^e$. Therefore to a good approximation the nighttime value of $\overline{P}$ will be given by Eq. (30) with $\cos 2\phi \to 0$. The daytime value is given by Eq. (30) with $\phi \to 0$ (no propagation in the Earth), which in fact reproduces Eq. (18) when $P_x = 0$ (adiabatic propagation in the Sun). For detectors at lower latitudes (such as Kamiokande-II at 26° latitude) 2ϕ is larger and the averaging is even more complete.

To estimate the Earth effect on the allowed regions of Fig. 2(a), we consider a typical ^{8}B neutrino which is created at $r \approx 0.045 r_{\rm Sun}$ ($N_n/N_e \approx 0.425$), and examine the difference between $\overline{P} = \frac{1}{2}(\overline{P}_{\rm day} + \overline{P}_{\rm night})$ and $\overline{P}_{\rm day}$ (no Earth effects). For the parameters within the solar solution shown in Fig. 2(a) the expected value of $\overline{P}$ can increase by as much as 0.06 when Earth effects are

included. From these estimates for the Earth-corrected probabilities, the dashed curves in Fig. 2(a) show the approximate shift in the allowed region due to ν_e regeneration in the Earth. We note that for $\epsilon_d < 0.01$ the mixing angle in Earth θ_m^e is small and the Earth effect is negligible.

Kamiokande-II has reported [2] no significant difference between daytime and nighttime signals

$$\frac{\text{Day} - \text{Night}}{\text{Day} + \text{Night}} = -0.08 \pm 0.11 \pm 0.03. \tag{32}$$

The predicted values of this ratio range from 0 to -0.11 in the region of parameters allowed by the solar data (after correcting for Earth effects). Therefore we conclude that the present day/night measurements do not exclude any part of the allowed regions, but that future measurements at the few percent level could exclude some or all of the region $\epsilon_d > 0.03$.

A comparison of summer and winter signals has been reported by the ^{37}Cl experiment [24]; they report no statistically significant difference. Due to averaging, the prediction for this difference is small in massless neutrino models with FCNC and new FDNC that explain the solar neutrino data.

For ν-u NC scattering, similar remarks apply. The mixing angle in the Earth is given by Eq. (29) with $d \to u$. The condition $0.40 < \epsilon'_u < 0.46$ for a resonance in the Sun is incompatible with a resonance in the Earth, but the denominator $(3\epsilon'_u - 1)$ in Eq. (29) is now smaller than in the ν-d case; however, the maximum value of ϵ_u in the numerator is also smaller, so the maximum Earth mixing angle is much the same as before. Therefore, in practice Earth effects on solar solutions with nonstandard ν-u scattering, shown by the dashed curves in Fig. 2(b), are very similar to Earth effects in the ν-d case.

For ν-e NC scattering, the mixing angle is the same in the Sun and in the Earth [Eq. (26)], but the cumulative phase ϕ in the Earth [given by Eq. (31)] is roughly two orders of magnitude smaller than the phase ψ in the Sun [given by Eq. (28)] because both the density and distance traveled are much smaller. Consequently, for the long-wavelength large-mixing solutions of Sec. II C, in which ψ in the Sun corresponds to a small, odd multiple of π, the cumulative phase ϕ in the Earth will lead to little day/night or summer/winter modulation.

E. Earth effects on atmospheric and accelerator neutrinos

Nonstandard NC scattering can also affect the fluxes of atmospheric ν_e, $\overline{\nu}_e$, ν_μ, and $\overline{\nu}_\mu$ neutrinos when they propagate through the Earth. The $\delta m^2 = 0$ scenario is unchanged if we replace neutrinos by antineutrinos (all forward scattering amplitudes change sign but the ratios ϵ_f and ϵ'_f are unchanged); also the propagation is independent of energy. Hence the general considerations in Sec. II D apply equally to the higher-energy neutrinos and antineutrinos of atmospheric origin.

If new NC interactions mix ν_e with ν_τ (favored over ν_e-ν_μ mixing; see Sec. V), then ν_μ and $\overline{\nu}_\mu$ fluxes will be unaffected. The up/down ratio of ν_e or $\overline{\nu}_e$ fluxes will be affected by $\nu_e \to \nu_\tau$ conversion in the Earth.

For solar solutions based on nonstandard ν-d NC scattering, the only cases with appreciable Earth effects are adiabatic solutions with large ϵ_d. As we have already seen, these solutions give moderate mixing and many oscillations for distances of order the Earth's diameter, so neutrinos coming upward from the antipodes will effectively be oscillation-averaged if they are accepted over a wide angle. The up/down ratio then measures

$$\left(\frac{\text{up}}{\text{down}}\right)_{\nu_e,\overline{\nu}_e} = 1 - \frac{1}{2}\sin^2 2\theta_m^e = 1 - \frac{18\epsilon_d^2}{36\epsilon_d^2 + (3\epsilon'_d - 1)^2}. \tag{33}$$

The Earth-corrected solutions of Fig. 2(a) then allow up/down ratios for ν_e and $\overline{\nu}_e$ fluxes in the range 0.93–1.00. In practice there would be a background of apparent ν_e and ν_μ events from $\nu_e \to \nu_\tau$ conversion followed by τ production and decay, but this would be suppressed by the $\tau \to \ell\overline{\nu}\nu$ branching fraction and the softer energy spectrum.

These oscillations are not large enough to explain why the μ/e ratio in upward events [25] at Kamiokande-II is 40% lower than expected [26]; in fact, for $\nu_e \to \nu_\tau$ oscillations this ratio would be increased.

For ν-u NC scattering, similar considerations apply and the up/down formula of Eq. (33) remains valid (after changing $d \to u$); the up/down ratio for ν_e and $\overline{\nu}_e$ fluxes can be as low as 0.95.

For ν-e NC scattering, the mixing angle is the same in the Sun and the Earth. However, as discussed in Sec. II D, the long-wavelength solutions that fit the solar data have wavelengths much longer than the Earth's diameter, so atmospheric neutrinos have too little distance to oscillate and the up/down ratios for all kinds of neutrinos are close to 1.

Oscillations in the Earth can also be probed using accelerator neutrino beams over long distances [27]. The ν-d and ν-u NC solar solutions that give the largest effects have Earth oscillation wavelengths of several thousand kilometers, which may be probed by very long-baseline terrestrial experiments. Furthermore, in the favored case of ν_e-ν_τ mixing, only the small ν_e component of the beam would be modulated, whereas the dominant ν_μ component would not. The ν-e NC solar solutions give negligible effects for long-baseline experiments; their wavelengths are too long.

III. MASSIVE NEUTRINOS: NO NEW FDNC

In this section we assume that δm^2 is significantly nonzero, and that the new neutral currents play a negligible role in the diagonal elements in Eq. (7), i.e.,

$$\epsilon'_e + 2\epsilon'_u + \epsilon'_d + (\epsilon'_u + 2\epsilon'_d)\frac{N_n}{N_e} \ll 1. \tag{34}$$

This scenario has been discussed in Ref. [4] (for no vacuum mixing) and Ref. [5] (with vacuum mixing).

The occurrence of an MSW resonance is determined by the standard model parameters

$$(N_e)_{\rm res} = \delta m^2 \cos 2\theta/(2\sqrt{2}G_F E_\nu). \quad (35)$$

In the off-diagonal elements, the standard contribution $\delta m^2 \sin 2\theta/(4E_\nu)$ is replaced by $B + \delta m^2 \sin 2\theta/(4E_\nu)$. The propagation matrix is therefore precisely that of the standard MSW problem, provided we make the substitutions

$$(\delta m^2)_{\rm MSW} = \delta m^2 \sqrt{\cos^2 2\theta + (b + \sin 2\theta)^2}, \quad (36)$$

$$(\tan 2\theta)_{\rm MSW} = (b + \sin 2\theta)/\cos 2\theta, \quad (37)$$

where the MSW subscripts represent parameters in the standard MSW solution and

$$b = 4BE_\nu/\delta m^2. \quad (38)$$

The only difference from the standard MSW evolution is that b depends on N_e and N_n, so that $(\delta m^2)_{\rm MSW}$ and $(\tan 2\theta)_{\rm MSW}$ are not constant during propagation. However, if both b and $\sin 2\theta$ are small then the resonance is narrow, and b will be approximately constant in the critical resonance region where the $\nu_e \to \nu_\alpha$ transition takes place. Thus, we can use the value of b at the resonance, which can be determined from the definition of b and Eq. (35):

$$b_{\rm res} = 2\cos 2\theta \left[\epsilon_e + 2\epsilon_u + \epsilon_d + (\epsilon_u + 2\epsilon_d)\left(\frac{N_n}{N_e}\right)_{\rm res}\right]. \quad (39)$$

If $\sin 2\theta$ is not small then the resonance is not narrow, but if b is small the fact that it varies in the resonance region has little effect on neutrino propagation. Since we generally expect that b will be small (it is proportional to the ϵ_f, which are restricted by other data), to a good approximation the oscillations should proceed as in the standard MSW effect for any value of $\sin 2\theta$, except that the MSW parameters are shifted according to Eqs. (36) and (37) with $b = b_{\rm res}$. The average oscillation probability for a neutrino of given energy and initial position is given by [9]

$$\overline{P}(\nu_e \to \nu_e) = \tfrac{1}{2}\left[1 + (1 - 2P_x)(\cos 2\theta)_{\rm MSW} \cos 2\theta^o_m\right], \quad (40)$$

where

$$\cos 2\theta^o_m = \frac{-[N^o_e/(N_e)_{\rm res} - 1]}{\sqrt{(\tan^2 2\theta)_{\rm MSW} + [N^o_e/(N_e)_{\rm res} - 1]^2}}, \quad (41)$$

and P_x is given by Eq. (19) with adiabaticity parameter

$$\gamma_c = \frac{(\delta m^2)_{\rm MSW}}{2E_\nu}\left(\frac{\sin^2 2\theta}{\cos 2\theta}\right)_{\rm MSW}\left|\frac{1}{N_e}\frac{dN_e}{dx}\right|^{-1}_{\rm res}. \quad (42)$$

The parameters $(\delta m^2)_{\rm MSW}$ and $(\tan 2\theta)_{\rm MSW}$ have an energy dependence from the $(N_n/N_e)_{\rm res}$ term in $b_{\rm res}$, but it is small since N_n/N_e does not change much in the Sun.

A. ν-d FCNC only

For ν-d scattering the resonance value of b is

$$b_{\rm res} = 2\epsilon_d \cos 2\theta \left[1 + 2\left(\frac{N_n}{N_e}\right)_{\rm res}\right]. \quad (43)$$

The 95% C.L. allowed region for the ^{37}Cl and K-II data in $(\delta m^2, \sin^2 2\theta)$ space is shown in Fig. 5 for $\epsilon_d = -0.05$ and 0.05; the standard MSW allowed region is also shown for comparison. In finding the allowed regions for nonzero ϵ_d we used the same method for calculating $\overline{P}(\nu_e \to \nu_e)$ as in our standard MSW calculation [12], except that the MSW parameters were shifted according to Eqs. (36) and (37) for each neutrino energy. Thus the slight energy dependence of $(N_n/N_e)_{\rm res}$ (and hence of $b_{\rm res}$), which occurs because the position of the resonance depends on E_ν, was included in our calculation.

In our calculation we have not included the effects of ν_e regeneration in the Earth; however, it should be very similar to the effect on the standard MSW allowed region, i.e., there is a bulge towards smaller $\sin^2 2\theta$ in the vertical part of the solution near $\delta m^2 = 3 \times 10^{-6}$ eV^2. Much of this area is ruled out by day/night measurements [2] at Kamiokande-II; the effect of this exclusion on the allowed region is shown in Fig. 5.

The changes in the allowed regions for nonzero ϵ_d seen in Fig. 5 may be easily understood by examining Eqs. (36) and (37). Positive ϵ_d (which makes $b_{\rm res}$ positive) has the effect of moving the allowed region towards smaller $\sin^2 2\theta$ since the smaller value of $\sin 2\theta$ is compen-

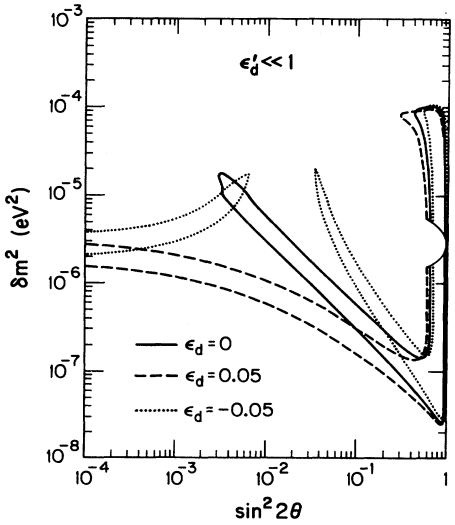

FIG. 5. Solutions to the solar puzzle for ν-d FCNC scattering with massive neutrinos and negligible new FDNC ($\delta m^2 \neq 0$ and $\epsilon'_d \ll 1$). The two cases ϵ_d=0.05 and −0.05 are indicated by dashed and dotted curves, respectively. In each case the corresponding curves enclose the region in $\delta m^2 - \sin^2 2\theta$ parameter space that fits the data of Eq. (21) within 95% C.L. The standard MSW solution ($\epsilon_d = 0$, solid curve) is also shown for comparison; the missing section of the vertical solution near $\delta m^2 = 3 \times 10^{-6}$ eV^2 is excluded by Kamiokande-II day/night measurements (Ref. [2]).

sated by the additional term $b_{\rm res}$ in Eq. (37) ($0 \leq \theta \leq \pi/2$ by convention). Likewise, the allowed region also shifts towards smaller δm^2 since the quantity inside the square root in Eq. (36) is larger than 1 and can compensate for a slightly reduced δm^2. Negative ϵ_d has the opposite effect, at least for the region $\sin^2 2\theta > |b_{\rm res}|^2$; the off-diagonal term changes sign and a mirror solution appears in the region $\sin^2 2\theta < |b_{\rm res}|^2$.

The predictions for ^{71}Ga experiments show similar changes from the standard MSW scenario; Fig. 6 shows contours of expected ^{71}Ga counting rates for $\epsilon_d = -0.05$ and 0.05. For positive ϵ_d, the predictions are shifted to lower $\sin^2 2\theta$ and δm^2 (the standard MSW predictions are depicted, e.g., in Fig. 12 of Ref. [9]). For negative ϵ_d the reverse occurs, and there are mirror contours for $\sin^2 2\theta < |b_{\rm res}|^2$. In the region near $\sin^2 2\theta = |b_{\rm res}|^2$ the contours merge because of the slight smearing effect from the E_ν dependence of $b_{\rm res}$. The shaded regions in Fig. 6 are the allowed regions from ^{37}Cl and K-II data from Fig. 5. The range of predictions for ^{71}Ga consistent with ^{37}Cl and K-II do not change from the standard MSW scenario since both the allowed region and the prediction contours shift in approximately the same way; there might be a very slight difference due to the different neutrino energies sampled in the experiments, but this effect is small.

Because massive neutrino oscillations involving FCNC mimic standard MSW oscillations, distinguishing between the two would be extremely difficult. Perhaps the best hope for verifying the existence of such FC interactions is with more direct tests, such as high-precision neutrino scattering experiments or improved searches for rare decays (see Sec. V for a discussion of the current limits).

B. ν-u FCNC only

In this case the resonance value of b is

$$b_{\rm res} = 2\epsilon_u \cos 2\theta \left[2 + \left(\frac{N_n}{N_e}\right)_{\rm res}\right]. \tag{44}$$

Otherwise, this case is similar to the previous one; $b_{\rm res}$ will be even less sensitive to the neutrino energy since the relative coefficient of $(N_n/N_e)_{\rm res}$ is smaller.

C. ν-e FCNC only

In this case the resonance value of b is

$$b_{\rm res} = 2\epsilon_e \cos 2\theta. \tag{45}$$

Since $b_{\rm res}$ does not depend on $(N_n/N_e)_{\rm res}$, it is independent of neutrino energy. Hence the allowed regions and prediction contours for future experiments may be found by directly applying the shift of Eqs. (36) and (37) to the corresponding curves for the standard MSW scenario [8–12].

IV. MASSIVE NEUTRINOS WITH FCNC AND NEW FDNC

In this section we assume that δm^2 and ϵ'_f are both non-negligible. Then the matrix equation for propagation through matter can be cast in the form

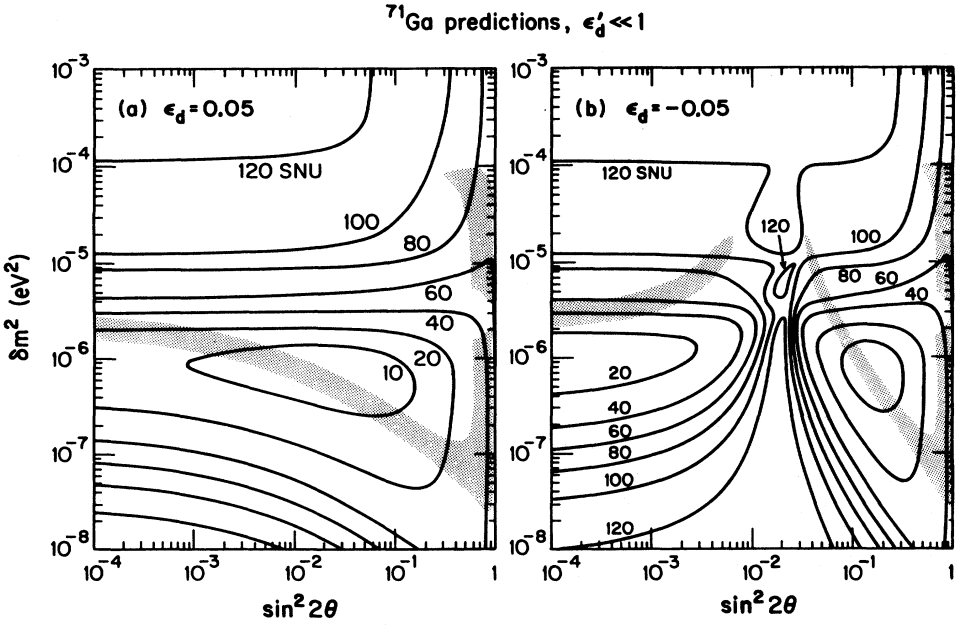

FIG. 6. Predictions for the solar neutrino counting rate in gallium detectors for the ν-d FCNC solutions of Fig. 5. The contours in the $\sin^2 2\theta$, δm^2 plane correspond to constant predicted rates in SNU, for the cases (a) $\epsilon_d = 0.05$ and (b) $\epsilon_d = -0.05$. The solution regions of Fig. 5 are indicated by shading.

$$i\frac{d}{dx}\begin{pmatrix}\nu_e\\ \nu_\alpha\end{pmatrix}=\begin{pmatrix}0 & \delta m^2(\sin 2\theta+b)/(4E_\nu)\\ \delta m^2(\sin 2\theta+b)/(4E_\nu) & \delta m^2\cos 2\theta/(2E_\nu)-\sqrt{2}G_F N_e^{\rm eff}\end{pmatrix}\begin{pmatrix}\nu_e\\ \nu_\alpha\end{pmatrix}, \tag{46}$$

where b is defined in Eq. (38) and

$$N_e^{\rm eff}=(1-\epsilon'_e-2\epsilon'_u-\epsilon'_d)N_e-(\epsilon'_u+2\epsilon'_d)N_n. \tag{47}$$

Making the substitutions defined in Eqs. (36) and (37), Eq. (46) has the same form as the standard MSW propagation with $N_e^{\rm eff}$ replacing N_e. In this way, it is similar to the sterile neutrino scenario (where $N_e^{\rm eff}=N_e-\frac{1}{2}N_n$) [14]; however, in this more general case $N_e^{\rm eff}$ depends on ϵ'_f. The resonance condition is

$$(N_e^{\rm eff})_{\rm res}=\delta m^2\cos 2\theta/(2\sqrt{2}G_F E_\nu). \tag{48}$$

We now examine the detailed behavior of resonance formation in the three NC scattering scenarios.

A. ν-d FCNC and FDNC only

If $N_e^{\rm eff}$ initially is negative, as may occur near the center of the Sun where N_n/N_e is larger, then the lower right diagonal element of the propagation matrix in Eq. (46) $[\delta m^2\cos 2\theta/(2E_\nu)+C]$ will be positive. In this case there is the possibility for one or even two resonance layers in the Sun. To see exactly how these resonance layers arise we show in Fig. 7 the value of the the lower right diagonal element of Eq. (46) in the Sun vs N_e for several sets of parameters, remembering that a resonance occurs when this element vanishes.

Figure 7(a) shows the lower diagonal element for $\delta m^2=0$; this is just the case described in Sec. II A. A resonance occurs for $0.50<\epsilon'_d<0.75$; for higher (lower) values the term is always positive (negative) and there is no resonance. In Figs. 7(b) and 7(c) a positive value of δm^2 is included, effectively raising the curves above their positions in Fig. 7(a). For values of ϵ'_d which had a resonance before, there are now either two resonances or none, depending on the size of δm^2 [Fig. 7(b)]. In Fig. 7(c) we see that for some values of ϵ'_d which were too small to induce a resonance when $\delta m^2=0$ (such as $\epsilon'_d=0.45$) there are now two resonances; for still smaller values (such as $\epsilon'_d=0.10$), there will be one resonance. The regions where no, one, or two resonances occur for ν-d FCNC scattering are summarized in Fig. 8(a).

Situations with a single resonance layer are similar to the scenarios in Sec. III. The oscillation probabilities may be calculated in the same way as in Sec. III A, except $N_e^{\rm eff}$ replaces N_e [i.e., by using Eqs. (36), (37), (39)–(42), (47), and (48) with $N_e^{\rm eff}\to N_e$ in Eqs. (41) and (42)]. With a non-adiabatic crossing far away from the center of the Sun, these scenarios would give predictions similar to standard MSW oscillations [after adjusting for the parameter shift in Eqs. (36) and (37)] since the adiabaticity parameter γ_c in Eq. (42) depends on the logarithmic gradient of the density, which is unchanged when N_e is replaced by $N_e^{\rm eff}$. For adiabatic or large-mixing propagation, where the mixing-angle in matter and the position of the resonance are important, scenarios with $N_e^{\rm eff}$ could give predictions different from standard MSW.

When two resonance layers are present, the first (innermost) resonance is principally caused by a change in the ratio N_n/N_e, while the second occurs when the effective density $N_e^{\rm eff}$ crosses the standard MSW critical density. If the propagation at the inner resonance is adiabatic, then no transition from one Hamiltonian eigenstate to another occurs there (although there is a transition in the flavor basis), and the calculation essentially reduces to the case with a single resonance layer and a single adi-

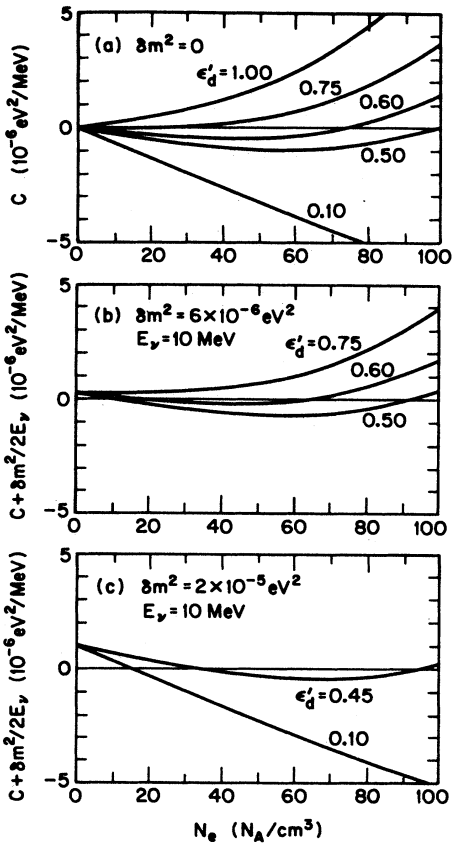

FIG. 7. Conditions for resonance in solar matter; comparison of ν-d FCNC examples. The vertical axis measures the lower right diagonal element of the propagation matrix in Eq. (7) [or equivalently Eq. (46)]; the vanishing of this element is the resonance condition. The horizontal axis measures the electron number density in units N_A/cm^3, running from 0 at the solar surface to approximately 100 at the core. The cases shown are (a) massless neutrinos ($\delta m^2=0$), with various examples of ϵ'_d, showing how only a limited range of ϵ'_d give a resonance in the Sun; (b) $\delta m^2=6\times10^{-6}\text{eV}^2$ and $E_\nu=10$ MeV, with different ϵ'_d; (c) $\delta m^2=2\times10^{-5}\text{eV}^2$ and $E_\nu=10$ MeV, with various ϵ'_d. The examples in (b) and (c) show how the introduction of nonzero δm^2 effectively displaces the curves relative to the massless case (a), leading to zero, one, or two resonances.

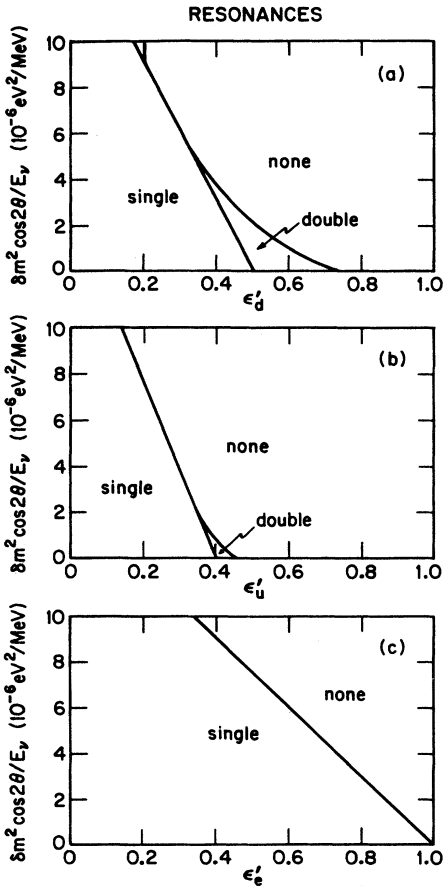

FIG. 8. The number of resonance layers in the Sun shown in the plane of relevant parameters for nonstandard (a) ν-d NC, (b) ν-u NC, and (c) ν-e NC. The segments of the horizontal axis beneath the double resonance regions have a single resonance layer.

abaticity parameter for the outer resonance. If the inner resonance is non-adiabatic, then two distinct adiabaticity parameters enter the calculation. We do not pursue this possibility any further.

B. ν-u FCNC and FDNC only

This case is very similar to ν-d FCNC only. The regions where zero, one, or two resonance layers occur vs ϵ'_u and $\delta m^2 \cos 2\theta / E_\nu$ are shown in Fig. 8(b). The determination of average oscillation probabilities proceeds as in Sec. IV A.

C. ν-e FCNC and FDNC only

Since $N_e^{\rm eff} = (1 - \epsilon'_e) N_e$ does not depend on N_n in this scenario, only one resonance layer is possible in the Sun. The regions where a resonance layer can occur vs ϵ'_e and $\delta m^2 \cos 2\theta / E_\nu$ are shown in Fig. 8(c). The determination of average oscillation probabilities proceeds as in Sec. IV A with one resonance layer.

V. LIMITS ON NEW NEUTRAL-CURRENT COUPLINGS

In this section we examine the limits on the flavor-changing and new diagonal couplings imposed by data. We first determine the model-independent limits that can be imposed on the $G^f_{\alpha\beta}$ in Eq. (4), and then examine the limits on interactions in supersymmetry models with broken R-parity described by the Lagrangian of Eqs. (10) and (11).

A. Model-independent limits

For the effective Lagrangian of Eq. (4), the most severe limits are from $\nu_\mu f \to \nu_\mu f$ scattering measurements. The left- and right-handed fermion couplings are

$$g^f_L = T^f_3 - Q^f x_{\rm w} + \tfrac{1}{2}(G^f_{\mu\mu V} - G^f_{\mu\mu A})/G_F,$$
$$g^f_R = -Q^f x_{\rm w} + \tfrac{1}{2}(G^f_{\mu\mu V} + G^f_{\mu\mu A})/G_F, \tag{49}$$

where T^f_3 and Q^f are the fermion weak isospin and electric charge, and $x_{\rm w} = \sin^2\theta_{\rm w}$. Limits on g^f_L and g^f_R from $\nu_\mu e$ and $\nu_\mu N$ deep inelastic scattering [28] give the individual constraints

$$G^e_{\mu\mu V}/G_F = -0.02 \pm 0.10,$$
$$G^d_{\mu\mu V}/G_F = -0.09 \pm 0.07, \tag{50}$$
$$G^u_{\mu\mu V}/G_F = -0.03 \pm 0.02.$$

We see that the $G^f_{\mu\mu V}$ are typically constrained to the $0.1 G_F$ level; hence the massless solar neutrino solution described in Sec. II with $\nu_e \to \nu_\mu$, which required $\epsilon'_f = (G^f_{\mu\mu V} - G^f_{eeV})/G_F$ to be 0.50–0.75 (0.40–0.46) for $d(u)$ quarks, can be realized only when G^f_{eeV} is negative and $|G^f_{eeV}| \gg |G^f_{\mu\mu V}|$ $(f = d, u)$.

The G^d_{ee} and G^u_{ee} couplings are constrained by deep inelastic ν_e-N scattering bounds [29], but these constraints are much looser than those from ν_μ-N scattering. For example, if we assume that CC scattering is given by the standard model and that nonstandard ν_μ scattering is negligible, the CHARM bound [29] on ν_e-N and $\bar{\nu}_e$-N NC scattering implies

$$\frac{(\frac{1}{2} - \frac{4}{3}x_{\rm w} + \frac{G^u_{eeV}}{G_F})^2 + (-\frac{1}{2} + \frac{G^u_{eeA}}{G_F})^2 + (-\frac{1}{2} + \frac{2}{3}x_{\rm w} + \frac{G^d_{eeV}}{G_F})^2 + (\frac{1}{2} + \frac{G^d_{eeA}}{G_F})^2}{(\frac{1}{2} - \frac{4}{3}x_{\rm w})^2 + (-\frac{1}{2})^2 + (-\frac{1}{2} + \frac{2}{3}x_{\rm w})^2 + (\frac{1}{2})^2} = 1.10 \pm 0.34. \tag{51}$$

For $x_w = 0.23$ and any mixture of ν-d and ν-u scattering, we obtain the model-independent bounds

$$-0.74 < G^d_{eeV}/G_F < 1.43, \quad -1.27 < G^u_{eeV}/G_F < 0.89, \tag{52}$$

at 95% C.L. These bounds become more severe if only ν-d or ν-u nonstandard NC contributes with couplings of specific chirality

$$-0.59 < G^d_{eeV}/G_F < 0.44, \quad -0.37 < G^u_{eeV}/G_F < 0.68 \quad (G_A = G_V), \tag{53}$$

$$-0.24 < G^d_{eeV}/G_F < 1.08, \quad -0.96 < G^u_{eeV}/G_F < 0.27 \quad (G_A = -G_V). \tag{54}$$

When combined with Eq. (50), these limits allow ϵ'_d and ϵ'_u to reach the critical values necessary for a $\nu_e \to \nu_\mu$ resonance in the Sun, except when the neutrino scatters predominantly off d_L ($G^d_{eeA} = -G^d_{eeV}$) or u_R ($G^u_{eeA} = G^u_{eeV}$) quarks.

Recent results from LAMPF [30] on low-energy elastic ν_e-e scattering [where $g^e_L \to g^e_L + 1$ in Eq. (49) due to an additional CC contribution] lead to the constraint

$$\tfrac{1}{2}\left[1 + 2x_w + (G^e_{eeV} - G^e_{eeA})/G_F\right]^2 + \tfrac{1}{6}\left[2x_w + (G^e_{eeV} + G^e_{eeA})/G_F\right]^2 = 1.15 \pm 0.21, \tag{55}$$

which translates into

$$-2.73 < G^e_{eeV}/G_F < 0.81 \quad \text{(any } G^e_{eeA}\text{)}, \tag{56}$$

$$-1.10 < G^e_{eeV}/G_F < 0.64 \quad (G^e_{eeA} = G^e_{eeV}), \tag{57}$$

$$-0.14 < G^e_{eeV}/G_F < 0.15 \quad (G^e_{eeA} = -G^e_{eeV}), \tag{58}$$

at 95% C.L. These limits allow $\epsilon'_e = (G^e_{\mu\mu V} - G^e_{eeV})/G_F$ to be near 1 (the critical value for maximal $\nu_e \to \nu_\mu$ mixing in the Sun), except when $G^e_{eeA} = -G^e_{eeV}$, i.e., ν_e scatters off e_L.

Since $\nu_\alpha f \to \nu_\beta f$ is experimentally indistinguishable from $\nu_\alpha f \to \nu_\alpha f$, limits may also be obtained on the off-diagonal terms $G^f_{\alpha\beta V}$ and $G^f_{\alpha\beta A}$. However, because the flavor-changing reactions add incoherently to the standard ones these limits are generally somewhat weaker, and they do not constrain any of the solar solutions. There are no experimental limits on the $G^f_{\tau\tau V}$ which contribute to $\nu_e \to \nu_\tau$ scenarios.

In summary, model-independent limits do not absolutely rule out $\nu_e \to \nu_\mu$ scenarios, but in any solar solution with non-negligible ϵ'_f the effective coupling G^f_{eeV} must be large and negative; particular chiral couplings are ruled out in some cases. There are no significant model-independent limits on $\nu_e \to \nu_\tau$ scenarios.

B. Limits on broken R-parity interactions

For the supersymmetric models with broken R parity, the couplings that can lead to the effective interaction of Eq. (4) are shown in Table I for the $\nu_e \to \nu_\mu$ and $\nu_e \to \nu_\tau$ cases. The couplings are listed in pairs; any given pair can generate both the flavor-changing and new diagonal currents [see, e.g., Eqs. (13) and (14)].

Limits on individual λ_{ijk} and λ'_{ijk} have been determined in Ref. [15]. In some cases rare flavor-changing processes give better limits on the product of two different couplings than the individual limits combined. For instance, $\mu \to e\gamma$ puts severe limits [4, 5, 31] on $\lambda_{131}\lambda_{231}$, $\lambda'_{1k1}\lambda'_{2k1}$ and $\lambda'_{11k}\lambda'_{21k}$. In Ref. [4], the process $\tau \to \rho^o e$ was used to constrain $\lambda'_{131}\lambda'_{331}$; this process can also be used to put limits on $\lambda'_{1k1}\lambda'_{3k1}$ and $\lambda'_{11k}\lambda'_{31k}$ for any k. These limits on the ϵ_f are summarized in Table II.

In the $\nu_e \to \nu_\mu$ scenarios the off-diagonal term ϵ_f is always very small, so that oscillations due to the flavor-changing interaction alone will be negligible. If the neutrinos are massive and have nonzero vacuum mixing, then the only difference from standard MSW oscillations will come from the the diagonal term ϵ'_f. Since it is of order $0.1G_F$ or less, there is no large effect on $N^{\rm eff}_e$ [see Eq. (47)]. Hence there are no sizeable nonstandard effects in the $\nu_e \to \nu_\mu$ scenario in the broken R-parity models.

For $\nu_e \to \nu_\tau$, nonzero λ'_{1k1}, λ'_{3k1} can give ϵ'_d large enough to cause a resonance in the Sun in the massless neutrino case (Sec. II). The corresponding limit on

TABLE I. Scenarios for flavor-changing neutral currents (FCNC) and flavor-diagonal neutral currents (FDNC) in supersymmetric R-parity violating models.

Scenario	Couplings	FCNC parameter	FDNC parameter
$\nu_e \to \nu_\mu$	$\lambda_{131}, \lambda_{231}$	$\epsilon_e = \lambda_{131}\lambda_{231}/(2m^2_{\tilde\tau_L})$	$\epsilon'_e = (\lvert\lambda_{231}\rvert^2 - \lvert\lambda_{131}\rvert^2)/(2m^2_{\tilde\tau_L})$
$\nu_e \to \nu_\mu$	$\lambda'_{1k1}, \lambda'_{2k1}$	$\epsilon_d = \lambda'_{1k1}\lambda'_{2k1}/(2m^2_{\tilde d^k_L})$	$\epsilon'_d = (\lvert\lambda'_{2k1}\rvert^2 - \lvert\lambda'_{1k1}\rvert^2)/(2m^2_{\tilde d^k_L})$
$\nu_e \to \nu_\mu$	$\lambda'_{11k}, \lambda'_{21k}$	$\epsilon_d = -\lambda'_{11k}\lambda'_{21k}/(2m^2_{\tilde d^k_R})$	$\epsilon'_d = (\lvert\lambda'_{11k}\rvert^2 - \lvert\lambda'_{21k}\rvert^2)/(2m^2_{\tilde d^k_R})$
$\nu_e \to \nu_\tau$	$\lambda_{121}, \lambda_{231}$	$\epsilon_e = -\lambda_{121}\lambda_{231}/(2m^2_{\tilde\mu_L})$	$\epsilon'_e = (\lvert\lambda_{231}\rvert^2 - \lvert\lambda_{121}\rvert^2)/(2m^2_{\tilde\mu_L})$
$\nu_e \to \nu_\tau$	$\lambda'_{1k1}, \lambda'_{3k1}$	$\epsilon_d = \lambda'_{1k1}\lambda'_{3k1}/(2m^2_{\tilde d^k_L})$	$\epsilon'_d = (\lvert\lambda'_{3k1}\rvert^2 - \lvert\lambda'_{1k1}\rvert^2)/(2m^2_{\tilde d^k_L})$
$\nu_e \to \nu_\tau$	$\lambda'_{11k}, \lambda'_{31k}$	$\epsilon_d = -\lambda'_{11k}\lambda'_{31k}/(2m^2_{\tilde d^k_R})$	$\epsilon'_d = (\lvert\lambda'_{11k}\rvert^2 - \lvert\lambda'_{31k}\rvert^2)/(2m^2_{\tilde d^k_R})$

TABLE II. Limits on flavor-changing neutral-currents (FCNC) and flavor-diagonal neutral-currents (FDNC) in supersymmetric R-parity violating models.

Scenario	Couplings	Limit on FCNC	Limit on FDNC
$\nu_e \to \nu_\mu$	$\lambda_{131}, \lambda_{231}$	$\lvert\epsilon_e\rvert < 1.5 \times 10^{-5}$ [b]	$-0.015 < \epsilon'_e < 0.012$ [a]
$\nu_e \to \nu_\mu$	$\lambda'_{1k1}, \lambda'_{2k1}$	$\lvert\epsilon_d\rvert < 1.5 \times 10^{-5}$ [b]	$-0.101 < \epsilon'_d < 0.073$ [a]
$\nu_e \to \nu_\mu$	$\lambda'_{11k}, \lambda'_{21k}$	$\lvert\epsilon_d\rvert < 1.5 \times 10^{-5}$ [b]	$-0.012 < \epsilon'_d < 0.001$ [a]
$\nu_e \to \nu_\tau$	$\lambda_{121}, \lambda_{231}$	$\lvert\epsilon_e\rvert < 5.4 \times 10^{-3}$ [a]	$-0.002 < \epsilon'_e < 0.012$ [a]
$\nu_e \to \nu_\tau$	$\lambda'_{1k1}, \lambda'_{3k1}$	$\lvert\epsilon_d\rvert < 8 \times 10^{-2}(m_{\tilde{u}^k_L}/m_{\tilde{d}^k_L})^2$ [c]	$-0.101 < \epsilon'_d$ [a]
$\nu_e \to \nu_\tau$	$\lambda'_{11k}, \lambda'_{31k}$	$\lvert\epsilon_d\rvert < 8 \times 10^{-2}$ [c]	$\epsilon'_d < 0.001$ [a]

[a] Ref. [15].
[b] $\mu \to e\gamma$ (Ref. [31]).
[c] $\tau \to \rho^o e$ (Ref. [4]).

ϵ_d is compatible with the entire region allowed by solar neutrino data [c.f. Fig. 2(a)]. Nonzero λ'_{1k1}, λ'_{3k1} or nonzero λ'_{11k}, λ'_{31k} can give ϵ_d large enough to affect the propagation in the massive neutrino cases (Secs. III and IV). Therefore, all of the ν-d NC scattering oscillation scenarios discussed earlier may be realized for $\nu_e \to \nu_\tau$ in the supersymmetric broken R-parity model. Finally, nonzero λ_{121},λ_{231} can give ϵ'_e as large as 0.012 and ϵ_e as large as 5.4×10^{-3}. Since $\epsilon'_e \ll 1$ it is not large enough to give large resonant effects in the sun, and the ϵ_e is not large enough to provide sufficient mixing in the absence of vacuum mixing [since from Eqs. (37) and (45) $(\sin^2 2\theta)_{\rm MSW} \approx 4\epsilon_e^2 \approx 1.2 \times 10^{-4}$]. Therefore ν-e NC scattering in the broken R-parity models does not give any new solar solutions.

Table II gives the direct limits on the couplings relevant to the effective Lagrangian for neutrino scattering in Eq. (4). There are many other limits from rare processes which put constraints on one of the λ or λ' in Table II in combination with a coupling not listed in the table. Some of these constraints can be severe. For example, there is a contribution to K_L-K_S mixing of

$$\Delta m_K = \frac{\lambda'_{k12}\lambda'_{k21}}{2(m_{\nu_{\tilde{k}L}})^2}\frac{2}{3}f_K^2 m_K \tag{59}$$

that leads to the bound

$$\frac{\lambda'_{k21}\lambda'_{k12}}{(m_{\tilde{\nu}_{kL}}/100\ \text{GeV})^2} < 9.3 \times 10^{-9}. \tag{60}$$

Similarly, requiring $\Delta M_B/\Gamma_B < 1$ in $B_d^o - \overline{B_d^o}$ mixing yields

$$\frac{\lambda'_{k31}\lambda'_{k13}}{(m_{\tilde{\nu}_{kL}}/100\ \text{GeV})^2} < 6 \times 10^{-8}. \tag{61}$$

If all the λ'_{ijk} are nonzero and of the same order of magnitude, then they must all be of the order 10^{-4} or less. This bound can be avoided if some of the couplings (such as λ'_{k13} and λ'_{k12} in the examples above) are more suppressed or vanish. Since there will be constraints from many other such reactions (e.g., rare decays), scenarios

TABLE III. Summary of scenarios with FCNC and new FDNC. The standard MSW scenario is shown for comparison, and the cases which may be realized in supersymmetric R-parity-violating (SUSY-RPV) models are identified.

δm^2, θ	FDNC	FCNC	New parameters	Comment
	√	√	ϵ'_q,ϵ_q	No vacuum osc. SUSY-RPV ($q = d$) [4]
	√	√	ϵ'_e,ϵ_e	Long-wavelength osc. in Sun
√			None	Standard MSW
√	√		None	MSW with sterile ν
√	√		ϵ'_f	MSW with $N_e^{\rm eff}$ SUSY-RPV ($f = d$)
√		√	ϵ_f	MSW with parameter shift SUSY-RPV ($f = d$) [4, 5]
√	√	√	ϵ'_f,ϵ_f	Two resonance layers possible SUSY-RPV ($f = d$)

with non-negligible couplings other than those listed in Table II must be very carefully examined to see if they are allowed by existing data.

VI. CONCLUSIONS

We have studied the possibility that the solar neutrino deficit may be due to 2-flavor ν_e-ν_α mixing in the Sun, mediated wholly or in part by new flavor-changing and flavor-diagonal neutral currents. The possible scenarios are listed in Table III. Our results may be summarized as follows.

(a) For $\delta m^2 = 0$ and ν-d or ν-u NC only, solar solutions exist in annular regions of the $(\epsilon'_f, \epsilon_f)$ plane, shown in Fig. 2.

(b) These solutions all depend on resonance crossing in the Sun; a resonance occurs in these scenarios if N_n/N_e crosses a critical value as it falls from about $\frac{1}{2}$ at the solar center to about $\frac{1}{6}$ at the surface. The lower horizontal band of solutions has non-adiabatic resonance crossing; the other solution regions are adiabatic. These solutions should be distinguishable from standard MSW oscillations since the amount of suppression depends only on the neutrino origin and not its energy; e.g., the suppression is uniform throughout the entire range 1.73 MeV $< E_\nu <$ 14 MeV, where essentially all neutrinos come from the ^{8}B process.

(c) Earth effects are most pronounced for the upper horizontal band of solutions. Here day/night asymmetries (for solar neutrinos) and up/down asymmetries (for atmospheric neutrinos) can reach the 5–10% level. The corresponding oscillation wavelengths in the Earth are of order several thousand kilometers, that could in principle be studied via long-baseline experiments using accelerator neutrino beams; but this assumes ν_e-ν_μ oscillations rather than ν_e-ν_τ.

(d) With $\delta m^2 = 0$ and ν-e NC only, mixing in the Sun is independent of radius, so there is no possibility of a resonance crossing. However, a special class of large-mixing long-wavelength solar solutions exists in this scenario. They must have ϵ'_e close to 1 with ϵ_e very small, so that centrally emitted ν_e will go through approximately $n + \frac{1}{2}$ oscillations on their way to the surface, with n small. Earth effects in these solutions are small.

(e) With $\delta m^2 \neq 0$ and $\epsilon'_f \ll 1$, new neutral currents play a role only in the off-diagonal elements of the propagation matrix. There is at most one resonance layer for each value of E_ν. This scenario can be related to standard MSW mixing by a simple shift of parameters. For the case of ν-d NC scattering we have shown in Fig. 5 how alternative choices $\epsilon_d = \pm 0.05$ displace the standard MSW solution region in the $(\sin^2 2\theta, \delta m^2)$ plane. Similar shifts occur for ν-u and ν-e NC scattering. These oscillation scenarios would be essentially indistinguishable from standard MSW oscillations, and would require more direct tests of the new NC interactions for identification.

(f) With $\delta m^2 \neq 0$ and ϵ'_f not negligible the condition for resonance in the Sun is modified in an essential way, so that resonances may occur in zero, one or two layers. This is illustrated in Fig. 7 for the case of ν-d NC. When two resonance layers occur, the inner resonance is principally caused by a change in the ratio N_n/N_e (and hence is analogous to the $\delta m^2 = 0$ cases), while the outer resonance is caused by the effective electron density crossing the usual MSW critical value. Thus this scenario combines the features of the massless and massive with $\epsilon'_f \ll 1$ scenarios.

(g) We have illustrated the predictions of the ν-d NC solutions for the ^{71}Ga detectors and for a proposed superfluid ^{4}He detector. Measurements with such detectors could severely constrain or even exclude these scenarios. For comparison, ^{4}He predictions for standard MSW oscillations are shown in Fig. 9.

(h) We have also considered Earth effects on solar neutrino, atmospheric neutrino and long-baseline accelerator neutrino fluxes. In the upper band of solutions of Fig. 2, day/night asymmetries for solar rates and up/down asymmetries for atmospheric rates can reach the 10% level; summer/winter asymmetries for solar neutrinos are smaller.

(i) There are model-independent bounds on nonstandard neutrino NC couplings in $\nu_e \to \nu_\mu$ scenarios; values of ϵ'_f of order 1 require $-G^f_{eeV}$ to be unnaturally much larger than $|G^f_{\mu\mu V}|$, and are ruled out for some chiral couplings. There are no significant model-independent limits on $\nu_e \to \nu_\tau$ scenarios.

(j) There are more stringent bounds on NC couplings in the specific framework of broken R-parity supersymmetry models; no $\nu_e \to \nu_\mu$ scenarios exist in which the FCNC couplings are large enough to give radically different solutions to the solar neutrino problem (slight modifications to the standard MSW solution are allowed). There are some limits on couplings in the $\nu_e \to \nu_\tau$ sector; they exclude ν-e NC solar solutions with $\delta m^2 = 0$ but allow ν-d NC solar solutions with resonant enhancement of massless and massive neutrino oscillations.

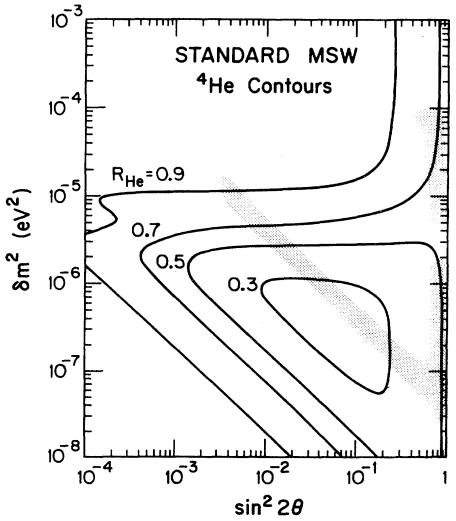

FIG. 9. Standard MSW predictions for the suppression ratio $R_{\rm He}$ in a superfluid helium detector. The 95% C.L. allowed region from the solid curves in Fig. 5 is denoted by shading.

ACKNOWLEDGMENTS

This work was supported in part by the U.S. Department of Energy under Contract No. DE-AC02-76ER00881 and Contract No. W-7405-Eng-82, Office of Energy Research (KA-01-01), Division of High Energy and Nuclear Physics, in part by the Texas National Research Laboratory Commission under Grant No. RGFY9173 and an SSC grant, and in part by the University of Wisconsin Research Committee with funds granted by the Wisconsin Alumni Research Foundation.

[1] R. Davis, Jr., in *Neutrino '88*, Proceedings of the XIXth International Conference on Neutrino Physics and Astrophysics, Boston, Massachusetts, 1988, edited by J. Schneps *et al.* (World Scientific, Singapore, 1989), p. 518.

[2] K.S. Hirata *et al.*, Phys. Rev. Lett. **63**, 16 (1989); **65**, 1297 (1990); **65**, 1301 (1990).

[3] J.N. Bahcall and R.K. Ulrich, Rev. Mod. Phys. **60**, 297 (1988).

[4] M.M. Guzzo, A. Masiero, and S.T. Petcov, Phys. Lett. B **260**, 154 (1991).

[5] E. Roulet, Fermilab Report No. FERMILAB-Pub-91/18-A (unpublished).

[6] L. Wolfenstein, Phys. Rev. D **17**, 2369 (1978); **20**, 2634 (1979).

[7] S.P. Mikheyev and A. Yu. Smirnov, Yad. Fiz. **42**, 1441 (1985) [Sov. J. Nucl. Phys. **42**, 913 (1985)]; Nuovo Cimento C **9**, 17 (1986).

[8] H.A. Bethe, Phys. Rev. Lett. **56**, 1305 (1986); V. Barger, R.J.N. Phillips, and K. Whisnant, Phys. Rev. D **34**, 980 (1986).

[9] W. Haxton, Phys. Rev. Lett. **57**, 1271 (1986); Phys. Rev. D **35**, 2352 (1987); S.J. Parke, Phys. Rev. Lett. **57**, 1275 (1986); S.T. Petcov, Phys. Lett. B **191**, 299 (1987); S. Toshev, Phys. Lett. B **198**, 551 (1988); T.K. Kuo and J. Pantaleone, Rev. Mod. Phys. **61**, 937 (1989).

[10] J.M. Gelb and S.P. Rosen, Phys. Rev. D **34**, 969 (1986); S.J. Parke and T. Walker, Phys. Rev. Lett. **57**, 2322 (1986); E.W. Kolb, M.S. Turner, and T.P. Walker, Phys. Lett. B **175**, 478 (1986); J. Bouchez *et al.*, Z. Phys. C **32**, 499 (1986); A. Dar *et al.*, Phys. Rev. D **35**, 3607 (1987); J.N. Bahcall and W.C. Haxton, *ibid.* **40**, 931 (1989); T.K. Kuo and J. Pantaleone, Rev. Mod. Phys. **61**, 937 (1989).

[11] J.N. Bahcall and H.A. Bethe, Phys. Rev. Lett. **65**, 2233 (1990); T.K. Kuo and J. Pantaleone, Mod. Phys. Lett. A **6**, 15 (1991); M. Fugugita and T. Yanagida, *ibid.* **6**, 645 (1991); A.B. Balantekin, A.J. Baltz, F. Loreti, S. Pakvasa, J. Pantaleone, and R.S. Raghavan, University of Hawaii Report No. UH-511-720-91, 1991 (unpublished).

[12] V. Barger, R.J.N. Phillips, and K. Whisnant, Phys. Rev. D **43**, 1110 (1991).

[13] C. Aulak and R. Mohapatra, Phys. Lett. **119B**, 136 (1983); F. Zwirner, *ibid.* **132B**, 103 (1983); L.J. Hall and M. Suzuki, Nucl. Phys. **B231**, 419 (1984); I.H. Lee, *ibid.* **B246**, 120 (1984); J. Ellis *et al.*, Phys. Lett. **150B**, 142 (1985); G.G. Ross and J.W.F. Valle, Phys. Lett. **151B**, 375 (1985); S. Dawson, Nucl. Phys. **B261**, 297 (1985); R. Barbieri and A. Masiero, *ibid.* **B267**, 679 (1986); S. Dimopoulos and L.J. Hall, Phys. Lett. B **207**, 210 (1987); P. Binetruy and J.F. Gunion, University of California at Davis Report No. UCD 88-32 (unpublished); S. Dimopoulos, R. Esmailzadeh, and L.J. Hall, Phys. Rev. D **41**, 2099 (1990).

[14] C.S. Lim and W.J. Marciano, Phys. Rev. D **37**, 1368 (1988); V. Barger, N. Deshpande, P.B. Pal, R.J.N. Phillips, and K. Whisnant, *ibid.* **43**, 1759 (1991).

[15] V. Barger, G.F. Giudice, and T.Y. Han, Phys. Rev. D **40**, 2987 (1989).

[16] SAGE experiment, V.N. Gavrin, in *Neutrino 90*, Proceedings of the 14th International Conference on Neutrino Physics and Astrophysics, Geneva, Switzerland, 1990, edited by J. Panam and K. Winter (North-Holland, Amsterdam, 1990).

[17] GALLEX experiment, T. Kirsten, in *Neutrino 90*, Proceedings of the 14th International Conference on Neutrino Physics and Astrophysics, Geneva, Switzerland, 1990, edited by J. Panam and K. Winter (North-Holland, Amsterdam, 1990).

[18] R.E. Lanou, H.J. Maris, and G.M. Seidel, Phys. Rev. Lett. **58**, 2498 (1987).

[19] V. Barger, R.J.N. Phillips, and K. Whisnant, Phys. Rev. D **24**, 538 (1981); Phys. Rev. Lett. **65**, 3084 (1990); S.L. Glashow and L.M. Krauss, Phys. Lett. B **190**, 199 (1987); A. Acker, S. Pakvasa, and J. Pantaleone, Phys. Rev. **D 43**, R1754 (1991).

[20] Sudbury Neutrino Observatory Proposal, SNO-87-12, 1987.

[21] T. Kajita, Tokyo Univ. Report No. ICR-185-89-2, 1989 (unpublished).

[22] R.S. Raghavan and S. Pakvasa, Phys. Rev. D **37**, 849 (1988).

[23] A.J. Baltz and J. Weneser, Phys. Rev. D **35**, 528 (1986); **37**, 3364 (1988); M. Cribier *et al.*, Phys. Lett. B **182**, 89 (1986); J. Bouchez *et al.*, Z. Phys. C **32**, 499 (1986); V.K. Ermilova, V.A. Tsarev, and V.A. Chechin, Pis'ma Zk. Eksp. Teor. Fiz. **43**, 353 (1986) [JETP Lett. **43**, 453 (1986)]; A. Dar and A. Mann, Nature **325**, 790 (1987); S. Hiroi *et al.*, Phys. Lett. B **198**, 403 (1987); Prog. Theor. Phys. **78**, 1428 (1987); J.N. Bahcall, J.M. Gelb, and S.P. Rosen, Phys. Rev. D **35**, 2976 (1987).

[24] M. Cribier *et al.*, Phys. Lett. B **188**, 168 (1987).

[25] Kamiokande-II experiment, T. Kajita, in *Proceedings of the XXVth International Conference on High Energy Physics*, Singapore, 1990, edited by K. K. Phua and Y. Yamaguchi (World Scientific, Singapore, 1991).

[26] G. Barr, T.K. Gaisser, and T. Stanev, Phys. Rev. **D 39**, 3532 (1989).

[27] A. Capone *et al.*, Nuovo Cimento **A98**, 211 (1987); R. Becker-Szendy *et al.*, Fermilab Proposal P815 (unpublished); Soudan II Collaboration, Fermilab Proposal P823 (unpublished); J. Pantaleone, Phys. Lett. B **246**, 245 (1990); R.H. Bernstein and S.J. Parke, Phys. Rev. D (to be published).

[28] U. Amaldi *et al.*, Phys. Rev. D **36**, 1385 (1987); G. Costa *et al.*, Nucl. Phys. **B297**, 244 (1988); P. Langacker and D. London, Phys. Rev. D **38**, 886 (1988), and references therein.

[29] BEBC WA66 Collaboration, H. Grassler *et al.*, Nucl. Phys. **B273**, 253 (1986); CHARM Collaboration, J. Dorenbosch *et al.*, Phys. Lett. B **180**, 303 (1986).

[30] R.C. Allen *et al.*, Phys. Rev. Lett. **64**, 1330 (1990).

[31] R. Barbieri *et al.*, Phys. Lett. B **252**, 251 (1990).